7th Canadian Conference on Earthquake Engineering / Montreal / 1995
7ième Conférence canadienne sur le génie paraséismique / Montréal / 1995

Dynamic Characteristics of Equipment in Sliding Structures[1]

L.-Y. Lu[2] and Y.-B. Yang[3]

ABSTRACT

The dynamic behavior of a single-DOF equipment mounted on a sliding primary structure is studied numerically. The equipment and the primary structure are treated as a combined sliding structural system subjected to harmonic ground motions. To deal with the discontinuity nature of sliding structural systems, in this work, a fictitious spring model is adopted. Based on the model, the problem is formulated in a state space form, and an incremental numerical scheme is proposed for computing the time history. Two numerical examples considering an equipment mounted on a single- and a multiple-DOF primary structures are given to study three effects, namely, the variation of the frictional coefficient of the sliding support, sub-harmonic effect on the mounted equipment, and tuning effect (i.e., when the frequency of the equipment is coincident with or close to that of primary structure). The dynamic characteristics of the mounted equipment are highlighted in the analysis of the two examples.

INTRODUCTION

Sliding structures are one kind of base-isolated structure systems. By implementing a sliding support under the base raft, a sliding structure can reduce the transmission of seismic excitation to its superstructure. Westermo and Udwadia'83 are among the first researchers to study a sliding system with an oscillating single DOF superstructure placed on a sliding foundation, and they have derived an analytical solution for the oscillator subjected to a harmonic ground motion. In their work, they have pointed out that the sliding system will possess a very special feature, called the sub-harmonic resonance, as can be identified by the fact that there are several resonant peaks in addition to the main peak associated with the main resonant frequency in the frequency response curve. Mostaghel and Tanbakuchi'83 and Mostaghel *et al.*'83 also studied a similar sliding system, using a semi-analytical solution procedure to compute the response caused by harmonic and earthquake ground excitations. Qamaruddin *et al.*'86 proved experimentally the effectiveness of using sliding supports for seismic protection of masonry buildings. In order to study multiple DOF sliding structure systems, Yang *et al.*'90 introduced a fictitious spring to represent the friction effect of the sliding device, and their result shows that the sliding device is effective in reducing the response of MDOF structures as well. It is well known that the motion of a sliding structure may have two different phases, namely, the sliding and non-sliding phases. While in each phase the sliding structure can be modeled as a linear system, the two phases have different governing equations. It is obvious that the overall behavior of the sliding structure is nonlinear. Due to this nonlineality, the sub-harmonic resonance is present in the frequency response

[1]This research is sponsored by the National Science Council of the Republic of China under Grant No. NSC 82-0410-E002-101.

[2]Associate Research Fellow, National Center for Research on Earthquake Engineering (NCREE), Taiwan, R. O. C.

[3]Head of Earthquake Simulation Division, NCREE. Also, professor of Department of Civil Engineering, National Taiwan University, Taipei, Taiwan, R. O. C.

of the sliding structure, thereby making the sliding structure become a very complicated structural system. While the effectiveness of sliding devices in seismic isolation has been studied by the previous authors, this work aims to investigate the dynamic behavior of an equipment item mounted on a sliding primary structure.

MATHEMATICAL MODEL AND FORMULATION

A sliding primary structure with an attached equipment can be considered as a combined structural system. In this work, the primary structure is assumed to be an n-story shear-type building structure and an equipment as a single-DOF system is attached to one of the floor slabs. Such a system may be represented by Figure 1. Other assumptions made in this study include (1) frictional mechanism is of the Coulomb type. (2) the frictional coefficient between the sliding surfaces remains constant throughout the motion of the structure. (3) only horizontal ground motions are considered.

In Figure 1, the combined structure has $n+2$ degrees of freedom. As mentioned earlier, a sliding structure may exhibit the sliding and non-sliding phases. In the non-sliding phase, there is no relative motion between base raft and the ground. This implies that the motion of base raft is identical to the ground motion. Therefore, the DOF associated with the base raft may be removed, leaving $n+1$ DOFs to the structural system. On the other hand, the total number of DOFs needed to describe the response of structural system in sliding phase remains as $n+2$. In numerical analysis, this disagreement on the number of DOFs due to the transition of the sliding structure from one phase to the other may cause certain inconveniences. To this end, this work adopts the fictitious spring model proposed by Yang *et al.*'90, and derives formulas for systematic analysis of the combined structural system. As was suggested by Yang *et al.*'90, the spring constant k_f of the fictitious spring is taken as zero for the sliding phase and as a very large value for the non-sliding phase. With this model, the DOF associated with the base raft is preserved throughout the entire analysis process. In the non-sliding phase, the internal force of the fictitious spring will automatically account for the actual static frictional force which is required to balance the inertial force exerted by the superstructure.

When the structure depicted in Figure 1 is subjected to a ground motion, its dynamic equation can be expressed as

$$\mathbf{M}\ddot{\xi} + \mathbf{C}\dot{\xi} + \mathbf{K}\xi = -\mathbf{M}\mathbf{1}\ddot{x}_0 + \mathbf{f} \quad (1)$$

where the $(n+2)x1$ column matrix $\xi = \{\xi_1, \xi_2, \dots, \xi_n, \xi_b, \xi_e\}^T$ contains the relative displacements of the story slabs as well as the relative displacement of the equipment to the ground, and the $(n+2)x(n+2)$ matrices **M**, **C**, and **K** are, respectively, the mass, damping and stiffness matrices for the combined structural system, taking into account the properties of the mounted equipment as well as the fictitous spring constant k_f. In Equation (1), there are two force terms on the right hand side. The first term $\mathbf{M}\mathbf{1}\ddot{x}_0$ represents the inertial force acting on each DOF due to the ground acceleration $\ddot{x}_0$, while the second term **f** is to account for the dynamic frictional force. The $(n+2)x1$ column matrices **1** and **f** may be expressed as

$$\mathbf{1} = \{1, 1, \cdots, 1\}^T \quad (2)$$

$$\mathbf{f} = \left\{0, 0, \cdots, 0, -sgn(\dot{\xi}_b)F_d\right\}^T \quad (3)$$

where the superscript "*T*" denotes matrix transportation, the symbol $sgn(\bullet)$ means the sign of $(\bullet)$, and F_d denotes the dynamic frictional force under the base raft, which is equal to the maximum static frictional force, denoted by F_{max}. The term **f** must be added in Equation (1), since in the sliding phase the spring constant k_f is taken as zero, in which case the fictitious spring provides no spring force for accounting for the constant dynamic frictional force.

Equation (1) can be further rewritten in a state space form, i.e.

$$\dot{\mathbf{x}} = \mathbf{A}\mathbf{x} + \mathbf{u} + \mathbf{p} \tag{4}$$

where $\mathbf{x} = \left\{\dot{\xi}^T, \xi^T\right\}^T$ and **A** is a *2(n+2)x2(n+2)* system matrix

$$\mathbf{A} = \begin{bmatrix} -\mathbf{M}^{-1}\mathbf{C} & -\mathbf{M}^{-1}\mathbf{K} \\ \mathbf{I} & \mathbf{0} \end{bmatrix} \tag{5}$$

The two force terms in equation (4), namely, **u** and **p**, can be explicitly written as

$$\mathbf{u} + \mathbf{p} = \begin{Bmatrix} -\mathbf{1}\ddot{x}_0 \\ \mathbf{0} \end{Bmatrix} + \begin{Bmatrix} \mathbf{M}^{-1}\mathbf{f} \\ \mathbf{0} \end{Bmatrix}$$

Equation (4) can be used to describe the response of the sliding structure, either in the non-sliding or sliding phase, provided that the following two constraints are imposed:

$$\mathbf{p} = \mathbf{0}, \ \textit{for non-sliding phase} \tag{6.a}$$

$$\mathbf{A}(k_f) = \mathbf{A}(0), \ \textit{for sliding phase} \tag{6.b}$$

Note that in Equation (6.b), the system matrix **A** is written as a function of k_f to signify the fact that all the elements except k_f in **A** remain unchanged throughout the entire motion of the structure.

NUMERICAL SCHEME

1. Discritized General Solution

Equation (4) is the equation for a linear time-invariant system. However, with the constraints (6.a) and (6.b) imposed, it actually represents two sets of equations for the two different phases of motion. Equations (4) and (6.a) together describe the structure in the non-sliding phase, while Equations (4) and (6.b) the sliding phase. As the sliding system may switch between these two phases at certain instants (to be discussed later), the entire behavior of a sliding system becomes highly non-linear. Nevertheless, within each phase of motion, the system represented by either Equations (4) and (6.a) or (4) and (6.b) is a linear one. It follows that time response solution can be denoted by

$$\mathbf{x}(t) = e^{\mathbf{A}(t-t_i)}\mathbf{x}(t_i) + \int_{t_i}^{t} e^{\mathbf{A}(t-\tau)}\left[\mathbf{u}(\tau) + \mathbf{p}\right]d\tau, \qquad t_i < t \le t_f \tag{7}$$

where $e^{\mathbf{A}t}$, called the transition matrix, is a matrix exponential function of **A** and t, and t_i, t_f and $\mathbf{x}(t_i)$ are, respectively, the starting time, ending time and initial conditions for the current phase. Note that the force vector **p** is not a function of time. Once the sliding system completes this phase, it will switch to the other phase and, then, t_f and $\mathbf{x}(t_f)$ become t_i and $\mathbf{x}(t_i)$ of the next phase. Equation (7) can be further rewritten in a incremental form, i.e.,

$$\mathbf{x}_{k+1} = e^{\mathbf{A}\Delta t}\mathbf{x}_k + \left(\int_0^{\Delta t} e^{\mathbf{A}\tau} d\tau\right)(\mathbf{u}_k + \mathbf{p}) \tag{8}$$

where Δt is the size of the chosen time step, and $\mathbf{x}_k$ and $\mathbf{u}_k$ denote the values of $\mathbf{x}(t)$ and $\mathbf{u}(t)$ at kth time step. Equation (8) states that the solution for the current step $\mathbf{x}_{k+1}$ can be computed from the solution of the last step $\mathbf{x}_k$, provided that the force term ($\mathbf{u}_k$+$\mathbf{p}$) remains constant in each time interval Δt.

2. Condition for Transition from Non-sliding Phase to Sliding Phase

When the static frictional force reaches its maximum value F_{max}, the system will start to slide. In the fictitious spring model, the static frictional force, denoted by F_s, is provided by the spring force of the fictitious spring. Therefore, the condition for the sliding system to transfer from non-sliding phase to sliding phase can be expressed as

$$F_s = k_f \cdot \varepsilon(t_0) = F_{\max} \tag{9}$$

where t_0 is the moment when the structure starts to slide, and $\varepsilon(t)$ is the elongation of the fictitious spring which is related to the relative displacement of base raft, denoted by ξ_b, by an added constant. The exact value of transition time t_0 may not be immediately obtained in the solution process. It is likely to happen that the spring force is less than F_{max} at the current time step, say t_k, while exceeding F_{max} at the next time step t_{k+1}. When this occurs, t_0 is confined within the time interval (t_k, t_{k+1}). In this case, one may employ numerical methods, such as bisection method or Newton's method, etc., to solve Equation (9) for the exact transition time t_0 to a desired accuracy.

3. Conditions for Transition from Sliding Phase to Non-sliding Phase

After the structure enters the sliding phase, it may return to the non-sliding phase whenever the following two conditions are satisfied:

$$\begin{aligned} &\dot{\xi}_b(t_0) = 0 \\ &F_s' = m_b\ddot{x}_0(t_0) - k_n[\xi_n(t_0) - \xi_b(t_0)] - c_n\dot{\xi}_n(t_0) \le F_{\max} \end{aligned} \tag{10}$$

where F_s' is an equivalent static frictional force required to balance the motion of the superstructure computed in the sliding phase, which can be obtained from the free body diagram of the base raft (see Figure 2), based on the fact that the base raft and the ground have the same acceleration and velocity (i.e., $\ddot{\xi}_b = \dot{\xi}_b = 0$). At the moment when the system enters the non-sliding phase, F_s' becomes the actual F_s and will be used as the initial frictional force. Using this initial value, the corresponding initial elongation $\varepsilon(t_i)$ of the fictitous spring and the initial relative displacement $\xi_b(t_i)$ of the base raft can be computed, and applied to the non-sliding phase that follows.

NUMERICAL RESULTS AND DISCUSSION

In order to study the equipment response, the aforementioned numerical method has been applied to the study of two examples. In the first case, the primary structure considered is a single story building, while in the second case, the primary structure is a 4-story building. For both cases a single-DOF equipment is mounted on the top of the building roof and harmonic ground acceleration $\ddot{x}_0 = 0.5g\ sin\Omega t$

is imposed. The study will be focused on three aspects, namely, the variation of frictional coefficients, sub-harmonic resonance effect and tuning effect.

Case 1. Equipment on a Single-DOF Structure

Some parameters for the structural properties are: mass of base raft m_b = 6 lb; mass of structure m_s = 2 lb; structural stiffness k_s = 78.96 lbf/in; mass ratio of equipment to structure m_e / m_s = 1/100; fictitious spring constant k_f = 10000 k_s; structural damping c_s = 1.26 $\text{lb}\cdot\text{sec}/\text{in}$ (equal to a damping ratio ζ_s = 5%); equipment damping ratio ζ_e = 5 %. Resulting from the above chosen parameters, the undamped natural frequency of the primary structure is ω_s = 1.0 Hz for the non-sliding phase, and is ω_s^* = 1.15 Hz for the sliding phase (hereafter, a star sign "*" on an entity signifies that the entity is associated with the sliding phase).

In order to study the effect of variation of frictional coefficients, Figure 3 is plotted with four different frictional coefficients, namely, μ = 0.4, 0.25, 0.1 and 0.05, assuming the equipment frequency to be ω_e = 5 Hz. Four observations can be made from this figure: (1) The use of a smaller frictional coefficient generally will reduce the acceleration response of the equipment from the fixed base case. (2) Besides the main resonant response, there are extra peaks appearing in the range of lower excitation frequencies. These are nothing but the response of sub-harmonic resonance. With a large frictional coefficient, e.g., μ = 0.25 or 0.4, the sub-harmonic resonant response may exceed the response of a fixed base case. (3) The main resonant frequency associated with the natural frequency of the primary structure drifts from ω_s toward ω_s^*, as the values of μ changes from ∞(for fixed base case) toward 0.05, while the sub-harmonic resonant frequencies do not vary with μ.

From Figure 3, one may also note that sub-harmonic resonance only occurs at frequencies lower than the equipment's natural frequency. This can be more clearly observed in Figure 4, in which both structure and equipment responses are depicted for the case of μ = 0.1 and ω_e = 0.5 Hz. In the figure, it is observed that the equipment exhibits a very different sub-harmonic behavior from that of the primary structure.

With regard to the tuning effect, i.e., when the frequencies of the equipment and structure are very close, a case with ω_e= 1.1 Hz is considered and the result is depicted in Figure 5. The frequency ω_e=1.1 Hz is chosen so that ω_e falls between ω_s and ω_s^* (the natural frequencies of the non-sliding phase and sliding phase). Comparing Figure 5 (tuning case) with Figure 3 (non-tuning case), one may conclude that when ω_e is close to the structure's natural frequencies, the equipment responses at main resonance frequency (around 1.1 Hz) and also at sub-harmonic resonance frequencies are significantly amplified. Figure 6 illustrates how the equipment response varies with ω_e, when the ground frequency Ω is fixed at 0.5 Hz. It is observed that the effect of sub-harmonic resonance causes the response to be amplified when ω_e is tuned to around 1.3 Hz which results in a ratio of Ω/ω_e around 0.38 (a similar ratio of Ω/ω_e for the first sub-harmonic frequency in Figure 5). In order to study how the sub-harmonic resonance of the primary structure affects the equipment when the equipment is tuned through the primary structure's sub-harmonic resonant frequencies, it is assumed that both Ω and ω_e are equal and varied simultaneously, as in Figure 7. It can be observed that although the response of the primary structure exhibits several sub-harmonic peaks below 1 Hz, the equipment response will not be amplified when the equipment is tuned to these sub-harmonic resonant frequencies. However, it will be amplified when tuned to the structure's main resonant frequency, which falls between ω_s (1 Hz) and ω_s^* (1.15 Hz).

Case 2. Equipment on a 4-Story Structure

The response of an equipment mounted on a 4-story sliding structure is also investigated in this study. The structural properties are assumed as: mass of base raft m_b = 6 lb; mass of each story $m_1 = m_2 = m_3 = m_4$ = 2 lb; stiffness of each story $k_1 = k_2 = k_3 = k_4$ = 78.96 lbf/in; damping of each story $c_1 = c_2 = c_3 = c_4 = 1.26\ \mathrm{lb \cdot sec / in}$; mass ratio of equipment to structure m_e / m_1 = 1/100; fictitious spring stiffness $k_f = 10000\ k_1$; equipment damping ratio ζ_e = 5 %. The undamped natural frequencies of the primary structure, resulting from the above structural properties, have been listed in Table 1.

The effect of variation of the frictional coefficient on the equipment response is illustrated in Figure 8, in which μ = 0.25, 0.1 and 0.05 are considered. In general, the less value of μ, the smaller the response is. Also, the first main resonance frequency drifts from ω_1 (0.35 Hz) toward ω_1*(0.49 Hz), when μ decreases. In Figure 9, the equipment responses for the cases of ω_e = 1 Hz and 2.5 Hz are compared. Also shown in the figure is the response of the 4th-story roof, where the equipment is mounted. The case of ω_e = 1 Hz represents a tuned case (tuned to ω_2). Three observations can be made from the figure: (1) The tuned case has more sub-harmonic frequencies than the primary structure has. (2) Responses at both main and sub-harmonic resonant frequencies, are magnified in the tuned case. (3) For an equipment with higher natural frequency, i.e., relatively stiff, such as the case of ω_e = 2.5 Hz, it behaves like a rigid system. In this case, the equipment response curve is very similar to the response of the structure to which it is mounted. In order to investigate the tuning effect when the equipment frequency coincides with the sub-harmonic resonance frequencies of the primary structure, it is assumed that both Ω and ω_e are equal and varied simultaneously, as in Figure 10. It can be seen that although the response of the primary structure exhibits several sub-harmonic resonant peaks below 0.49 Hz, the response of the equipment is not amplified at these resonant frequencies. Nevertheless, the amplification of the response will occur when ω_e is tuned to the structure's main resonant frequencies. These main resonant frequencies are somewhere in between ω_i and ω_i^*, where i = 1, 2, and 3.

CONCLUSIONS

In order to study the dynamic behavior of single DOF equipments mounted on sliding primary structures subjected to harmonic ground motions, two numerical examples have been prepared. From the examples, the major observations are: (1) In general, the use of a sliding foundation is effective in reducing the equipment responses. However, due to the presence of sub-harmonic resonance, the equipment responses at the sub-harmonic resonant frequencies are higher than those of the fixed-base case if a larger frictional coefficient is adopted. (2) The sub-harmonic resonance will occur only when the excitation frequencies are lower than the equipment frequency. (3) When the equipment is tuned to the main resonant frequencies of the primary structure, the equipment response, compared with the un-tuned case, will be magnified at both main and sub-harmonic resonant frequencies. (4) The resonant frequencies vary with the selection of frictional coefficients.

REFERENCES

Mostaghel, N., Hejazi M., and Tanbakuchi, J. 1983. "Response of sliding structures to harmonic support motion," *Earthquake Engrg. Struct. Dyn.*, 11, 355-366.

Mostaghel, N., and Tanbakuchi, J. 1983. "Response of sliding structures to earthquake support motion," *Earthquake Engrg. Struct. Dyn.*, 11, 729-748.
Qamaruddin, M., Rasheeduzzafar, Arya, A. S., and Chandra, B. 1986. "Seismic response of masonry buildings with sliding substructure," *J. Struct. Engrg., ASCE*, 112(9), 2001-2011.
Westermo, B., and Udwadia, F. 1983. "Period response of a sliding oscillator system to harmonic excitation," *Earthquake Engrg. Struct. Dyn.*, 11, 135-146.
Yang, Y. B., Lee, T. Y., and Tsai, I. C. 1990. "Response of multi-degree-of-freedom structures with sliding supports," *Earthquake Engrg. Struct. Dyn.*, 19, 739-752.

Table 1 Undamped Natural Frequencies of the 4-Story Primary Structure

Non-Sliding Phase+ (Hz)				Sliding Phase++ (Hz)			
ω_1	ω_2	ω_3	ω_4	ω_1^*	ω_2^*	ω_3^*	ω_4^*
0.35	1.00	1.53	1.88	0.49	1.06	1.55	1.88

+ does not include the fictitious spring mode (about 57 Hz).
++ does not include the rigid body mode (0 Hz).

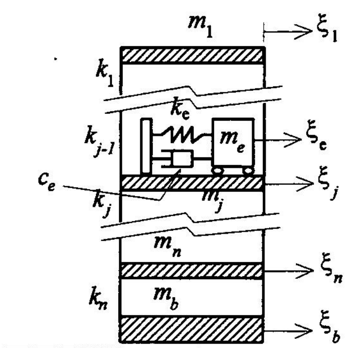

Figure 1 A Combined Equipment and Sliding Structural System

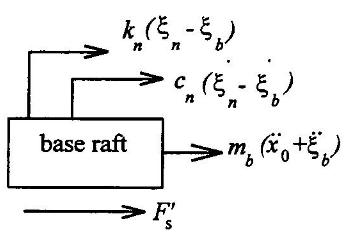

Figure 2 Free Body Diagram of Base Raft

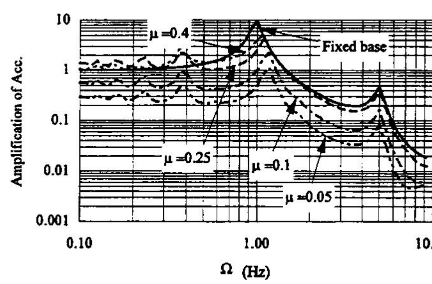

Figure 3 Effect of Frictional Coefficient μ ($\omega_e = 5$ Hz)

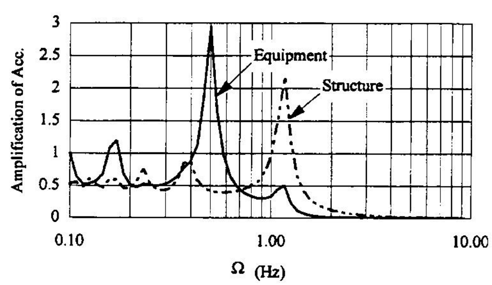

Figure 4 Comparison of Structure and Equipment Frequence Responses ($\omega_e = 0.5$ Hz; $\mu = 0.1$)

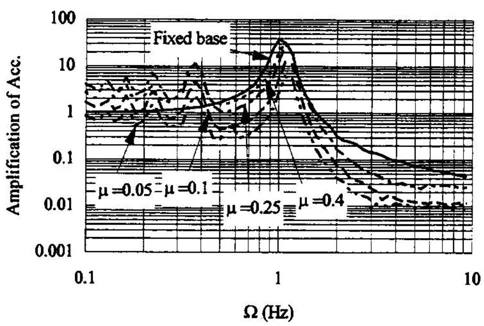

Figure 5 Frequency Response of Equipment When Tuned to the Structure Frequency (ω_e = 1.1 Hz)

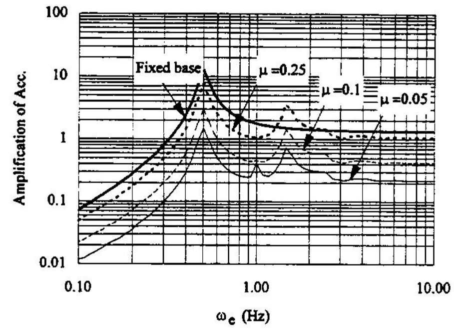

Figure 6 Study of Tuning Effect by Varying Equipment Frequency (Ω = 0.5 Hz)

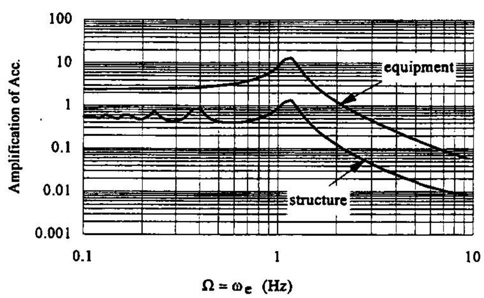

Figure 7 Study of Tuning Effect by Varying Ground and Equipemnt Frequencies Simultaneously (μ = 0.1)

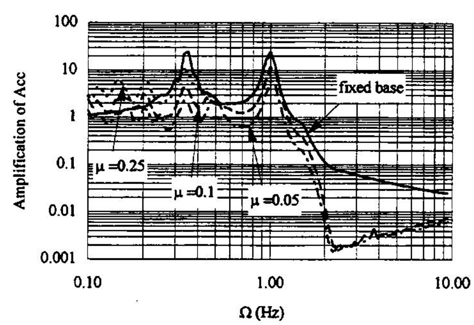

Figure 8 Effect of Frictional Coefficient on Equipment Response (ω_e = 1 Hz)

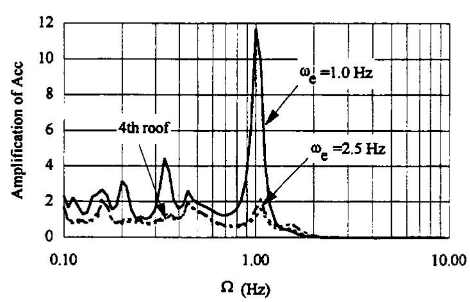

Figure 9 Comparison of Equipment Responses for Different Equipment Frequencies (μ = 0.1)

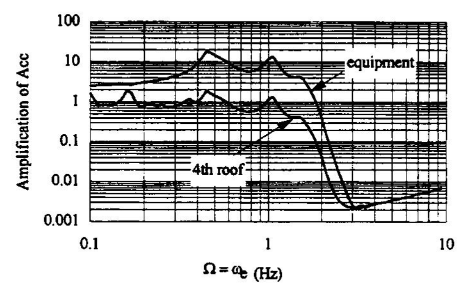

Figure 10 Study of Tuning Effect by Varying Ground and Equipemnt Frequencies Simultaneously

(μ = 0.1)